UC Irvine
UC Irvine Previously Published Works

Title
Spatial characteristics of thunderstorm rainfall fields and their relation to runoff

Permalink
https://escholarship.org/uc/item/5wg571vp

Journal
Journal of Hydrology, 271(1-4)

ISSN
0022-1694

Authors
Syed, Kamran H
Goodrich, David C
Myers, Donald E
et al.

Publication Date
2003-02-01

DOI
10.1016/s0022-1694(02)00311-6

Copyright Information

Peer reviewed

ELSEVIER

Spatial characteristics of thunderstorm rainfall fields and their relation to runoff

Kamran H. Syed[a,*,4], David C. Goodrich[b,1], Donald E. Myers[c,2], Soroosh Sorooshian[a,3]

[a]*Department of Hydrology and Water Resources, University of Arizona, Tucson, AZ, USA*
[b]*USDA-ARS Southwest Watershed Research Center, Tucson, AZ, USA*
[c]*Mathematics Department, University of Arizona, Tucson, AZ, USA*

Abstract

The main aim of this study was to assess the ability of simple geometric measures of thunderstorm rainfall in explaining the runoff response from the watershed. For calculation of storm geometric properties (e.g. areal coverage of storm, areal coverage of the high-intensity portion of the storm, position of storm centroid and the movement of storm centroid in time), spatial information of rainfall is needed. However, generally the rainfall data consists of rainfall depth values over an unevenly spaced network of raingauges. For this study, rainfall depth values were available for 91 raingauges in a watershed of about 148 km^2. There was a question about which interpolation method should be used for obtaining uniformly gridded data. Therefore, a small study was undertaken to compare cross-validation statistics and computed geometric parameters using two interpolation methods (kriging and multiquadric). These interpolation methods were used to estimate precipitation over a uniform 100 m × 100 m grid. The cross-validation results from the two methods were generally similar and neither method consistently performed better than the other did. In view of these results we decided to use multiquadric interpolation method for the rest of the study. Several geometric measures were then computed from interpolated surfaces for about 300 storm events occurring in a 17-year period. The correlation of these computed measures with basin runoff were then observed in an attempt to assess their relative importance in basin runoff response. It was observed that the majority of the storms (observed in the study) covered the entire watershed. Therefore, it was concluded that the areal coverage of storm was not a good indicator of the amount of runoff produced. The areal coverage of the storm core (10-min intensity greater than 25 mm/h), however, was found to be a much better predictor of runoff volume and peak rate. The most important variable in runoff production was found to be the volume of the storm core. It was also observed that the position of the storm core relative to the watershed outlet becomes more important as the catchment size increases, with storms positioned in the central portion of the watershed producing more runoff than those positioned near the outlet or near the head of the watershed. This observation indicates the importance of interaction of catchment size and shape with the spatial storm structure in runoff generation. Antecedent channel wetness was found to be of some importance in explaining runoff for the largest of the three

* Corresponding author. Fax: +1-775-458-3155.
  E-mail addresses: syed@atmos.umd.edu (K.H. Syed), dgoodrich@tucson.ars.ag.gov (D.C. Goodrich), myers@math.arizona.edu (D.E. Myers), soroosh@hwr.arizona.edu (S. Sorooshian).

[1] Fax: +1-520-670-5550.
[2] Fax: +1-520-621-8322.
[3] Fax: +1-520-621-1422.

[4] Present address : Department of Biological Sciences, University of Letnbridge, Letnbridge, Alberta, Canada.

watersheds studied but antecedent watershed wetness did not appreciably contributed to runoff explanation.
© 2002 Elsevier Science B.V. All rights reserved.

1. Introduction

In many semiarid regions the majority of the runoff is produced from extremely variable, high intensity, short duration rainfall events. An understanding of the space − time structure of these rainfall fields is of interest for storm modeling, runoff production and subsequent hydraulic structural design. In this study the space − time characteristics of rainfall fields (derived from a dense raingauge network) and their relationships to runoff were studied. Motivation for this study also stems from several results in the literature, which conclude that simpler rainfall–runoff models perform equally well as more complex models (Loague and Freeze, 1985; Michaud and Sorooshian, 1994a; Grayson et. al, 1992). While Goodrich (1990) found that the relatively complex research version of the KINEROS model (Woolhiser et al., 1990) made very good runoff predictions for four watersheds at small scales ($<$ 631 ha) the same model applied to the 148 km^2 Walnut Gulch Experimental Watershed did not provide accurate runoff predictions. At both the large (Michaud and Sorooshian, 1994b) and small scale (Goodrich, 1990; Faurès et al., 1995) the noted studies pointed out that significant errors in runoff prediction result from the misrepresentation of the rainfall field in time and space (see Woolhiser, 1996 for additional reasons for the loss of model accuracy at larger scales). Indeed, Goodrich (1990) noted that model runoff prediction errors from using one versus two raingauges were greater than the errors resulting from simplifying the watershed representation from 235 kinematic model elements to a single element in a 4.4 ha catchment. Given the importance of rainfall field characteristics and the findings that simple models often perform as well as complex runoff models at the large scale we were prompted to investigate whether more detailed descriptions of rainfall fields derived from a dense raingauge network would explain as much variability in runoff via simple regression (a very simple runoff model) or more complex model was warranted. To derive detailed rainfall space − time characteristics, the values of rainfall in a reasonably continuous spatial field are required. However, storm observations usually consist of widely scattered raingauge observations. The aim in this research was to avoid point statistics, inspired by a conclusion of Smith and Schreiber (1973, 1974). They pointed out that due to the scattered nature of summer thunderstorm cells, point statistics alone were inadequate to describe rainfall input within even a small area. To compute areal storm statistics, point rainfall data from multiple locations in a watershed must be processed to obtain rainfall estimates on a uniform grid via interpolation techniques. Numerous methods exist for the interpolation of point data. Among them are Thiessen polygon, polynomial interpolation, reciprocal distance, inverse square distance, optimal interpolation, trend surface, spline interpolation, multiple discriminant analysis, multiple linear regression and the normal ratio method.

These methods are described and practically applied by several authors (for example see Thiessen, 1911; Mandeville and Rodda, 1970; Shaw and Lynn, 1972; Lee et al., 1974; Kruizinga and Yperlaan, 1978; Creutin and Obled, 1982; Bastin et al., 1984; Tabios and Salas, 1985; Barendregt, 1987; Lebel et al. 1987; Supachai, 1988; Seed and Austin, 1990; Kwaadsteniet, 1990; Young, 1992; Abtew et al., 1993; Pegram and Pegram, 1993; Amani and Lebel, 1997; Goovaerts, 2000). Creutin and Obled (1982) showed that in a region with intense and strongly varying rainfall events, sophisticated techniques (e.g. spline surface fitting, optimal interpolation, kriging etc.) provide a much better estimation than any of the more commonly used techniques (nearest neighbor or arithmetic mean). Similar observations were made in several other independent studies (Shaw and Lynn, 1972; Tabios and Salas, 1985; Abtew et al., 1993). In view of these conclusions, it was decided to restrict the comparative study to assessing the performance of kriging and multiquadric methods

before performing spatial interpolation using a large data set. This exercise was essential in view of the amount of data to be processed (17 years of rainfall data from 91 raingauges). Moreover, few studies were found (at the time this study was undertaken i.e. 1993–94) which directly compared the performance of these two interpolation methods. Borga and Vizzaccaro (1997) have published an interesting study comparing these interpolation methods. The authors establish formal equivalence between multiquadric and kriging methods. However, they used radar data for estimation of rainfall. Similarly, the nature of data used by the other investigators was different from the type and resolution utilized in this study. For example, Shaw and Lynn (1972) only considered bi-cubic spline and multiquadric methods. Tabios and Salas (1985) and Abtew et al. (1993), on the other hand, compared the performance of several interpolation methods including kriging and multiquadric but used only annual precipitation data from widely scattered raingauges (Tabios and Salas, 1985) or monthly rainfall data (Abtew et al., 1993). Creutin and Obled (1982) used total rainfall depth during entire events but did not consider the multiquadric method. Supachai (1988) performed a detailed comparison of the performance of kriging and multiquadric methods but did not use rainfall data. The study of Goovaerts (2000) was distinct in that the author incorporated elevation information in the interpolation process. Goovaerts used kriging techniques and compared the results with those from more simple methods like Thiessen polygon and inverse distance square. The network of observation points was far less dense (36 stations in an area of 5000 km^2) than that used in this study (91 stations in an area of 148 km^2). It was observed that the kriging scheme which ignored elevation was better than the linear regression when the correlation was smaller than 0.75. In view of this topography was not considered for this study as Reich and Osborn (1982) found that rainfall events occurred randomly over the Walnut Gulch Experimental Watershed and noted a distinct lack of correlation with gauge elevation. Amani and Lebel (1997) also used very low gauge densities (40 and 100 km^2 per gauge) to compare langrangian and eulerian approaches. They

found langrangian kriging approaches to perform far better than the eulerian approaches.

The preceding discussion leads us directly to the specific objectives of this study, namely:

1. To compare the cross validation statistics and selected rainfall geometric parameters computed using kriging and multiquadric interpolation methods on convective rainfall (real and synthetic) data;
2. To characterize the nature of convective rainfall cells via several geometric storm parameters;
3. To evaluate the ability of geometric measures to explain basin runoff response (runoff volume and runoff peak rate); and,
4. To assess if incorporation of antecedent watershed and channel wetness can enhance runoff predictions provided by the rainfall geometric measures.

A description of the study area and the methodology used to achieve the above objectives are discussed first. A brief description of kriging and multiquadric methods is then presented, followed by the evaluation procedure used to assess interpolation performance. Then we describe how interpolated data were used to compute spatial storm parameters and how they were correlated to the runoff data. The results section discusses the performance of kriging and multiquadric interpolators and the relationship of observed thunderstorm rainfall properties to basin runoff.

2. Methodology

The study site for this research is the 148 km^2 USDA-ARS Walnut Gulch Experimental Watershed near Tombstone, Arizona (Fig. 1). The climate is semiarid and convective summer airmass thunderstorms produce virtually all of the runoff in the summer months of July, August and September by infiltration excess (Renard et al., 1993). The watershed is equipped with 91 weighing recording raingauges distributed over the watershed (Fig. 2). The watershed is divided into twelve primary subwatersheds; each equipped with precalibrated runoff measuring flumes (Fig. 1). Three watersheds

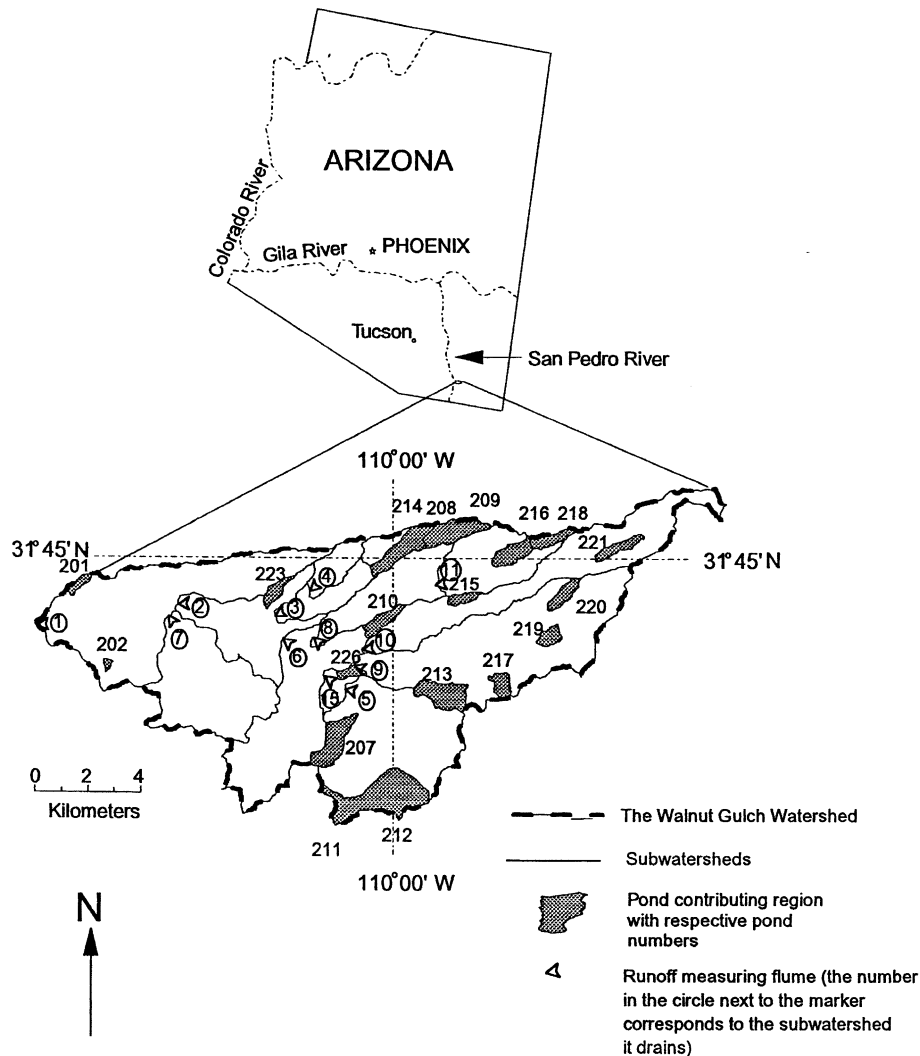# USDA-ARS WALNUT GULCH EXPERIMENTAL WATERSHED

Fig. 1. USDA ARS Walnut Gulch Experimental Watershed location map. Subwatersheds are delineated and regions contributing to the stock ponds are shaded (small numbers in blue refer to the pond numbers).

are the focus of this study. These are the entire Walnut Gulch (WG) Experimental Watershed (WG1; area = 148 km^2); subwatershed 6 (WG6; area = 93 km^2, and subwatershed 11 (WG11; 7.85 km^2). WG11 is characterized as small watershed and represents drainage from mainly grass dominated land. In this watershed approximately 20% of the area is dominated by desert shrub with a crown spread of approximately 30% cover and an understory of grasses. The area contributing runoff to two stockponds—pond 216 which is gauged and pond 218 which is ungauged—comprise the upper approximate one fourth of the subwatershed. WG6 drains about 65% of the upper portion of WG1 representing a mixed grass-brush land. Approximately 45% of area is covered with oak woodland and desert shrubs with
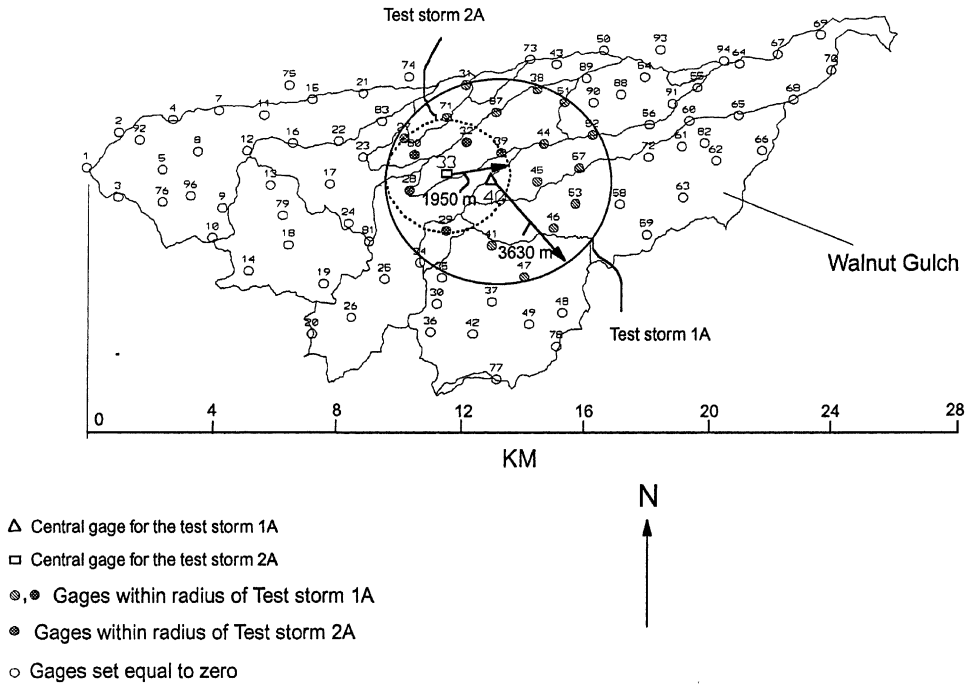
Fig. 2. Raingage locations, gauge numbers and illustration of analytic test storms.

a crown spread of 25%. The watershed contains 13 ponds comprising an area of about 1207 ha.

Interpolation methods and procedures to compare kriging to multiquadric are described first followed by description of methodology to derive geometric storm properties.

2.1. Interpolation methods to compute spatial rainfall characteristics

Kriging and multiquadric interpolation methods were selected for evaluation from review of prior research. In kriging (Journel and Huijbregts, 1978) the spatial correlation structure of observations is explicitly recognized and modeled via a variogram. This allows the prediction (interpolation) at unsampled locations via the following combination of linear equations:

$$z^*(x_p) = \sum_{i=1}^{n} \lambda_{pi} z(x_i) \tag{1}$$

where, z^* is the predicted value of the phenomenon at point x_p, z are the functional values at n number of

data points at locations x_i and λ are the kriging weights.

The kriging weights are obtained by minimizing the estimation variance. The minimum variance condition can be written in the form of a variogram to obtain the kriging system:

$$\gamma_{pj} = \sum_{j=1}^{n} \lambda_{pj} \gamma_{ij} + \mu_p \tag{2}$$

where, γ_{ij} is the variogram between the data points i and j; γ_{pj} is the variogram between the predicted point p and the data point j. The Lagrange multiplier μ_p appears because of the unbiasedness constraint below:

$$\sum_{i=1}^{n} \lambda_{pi} = 1. \tag{3}$$

By rewriting Eqs. (2) and (3) in matrix form a solution for the weighting coefficients can be obtained and

the regionalized variable at point p is predicted by

$$z^*(x_p) = [\lambda_{p1}, ..., \lambda_{pn} \mu_p] \begin{bmatrix} z(x_1) \\ \vdots \\ z(x_n) \\ 0 \end{bmatrix}. \qquad (4)$$

A computer package 'GEOEAS' (Englund and Sparks, 1990; Myers, 1991) was used for modeling of variograms and performing kriging computations.

The multiquadric method was developed by Hardy (1971), and is based on the minimum energy concept of mathematical physics (Supachai, 1988). In this technique, the surface is represented as a summation of many individual quadric surfaces. The value at any unsampled point is expressed as the sum of all the contributions from the quadric surfaces centered at all other data points (Shaw and Lynn, 1972).

Mathematically, the multiquadric system is formulated as follows. Every predicted point is affected by all the data points via the following equation:

$$F(p,q,r) = \sum_{j=1}^{n} \rho_j [c^2 + (p - p_j)^2 + (q - q_j)^2 + (r - r_j)^2]^{1/2} \qquad (5)$$

where, $F(p, q, r)$ represents a function on a Cartesian coordinate system (with coordinates p, q and r) that explains the magnitude of the phenomenon under consideration; defined with n data points and multiquadric coefficients ρ_j. The sum of the coefficients is forced to zero

$$\sum_{j=1}^{n} \rho_j = 0 \qquad (6)$$

to satisfy the minimum energy condition. Once the multiquadric coefficients are obtained using Eqs. (5) and (6) and observed data, the prediction (interpolation) of F at any location can be obtained via Eq. (5).

Note that the kriging predictor (Eq. (4)), can be rewritten in an equivalent form

$$z^*(x_p) = \sum_{i=1}^{n} b_i \gamma_{ip} + a \qquad (7)$$

where, $[b_1, ..., b_n, a]^T$ is the solution of the system with the same coefficient matrix as for the system to solve for the kriging weights (λ, see Eq. (2)). However, the right hand side (the column $[z(x_1), ..., z(x_2), 0]^T$) differs from Eq. (5). Hence the kriging predictor will look essentially the same as the multiquadric except for a different choice of the variogram. Note, however, that there is one important difference. In using the form of Eq. (4) one can use a moving neighborhood, but if the alternative form of Eq. (7) is used then one is essentially forced into using a unique neighborhood. The duality between the two methods has been further discussed by Myers (1994) and Borga and Vizzaccaro (1997).

We tested the performance of kriging and multiquadric methods for spatial rainfall interpolation mainly by comparing statistics of cross validation residuals. Two interpolation methods (kriging and multiquadric) were first compared on limited data. The data for comparison consisted of two artificial (synthetic) and one observed storm (occurring on July 30th, 1989) events. This storm event was chosen because of its distinct spatial character. The event had two storm cells operating at the two extreme ends of the watershed with 70 gauges reporting rain with total rainfall depths ranging from 1 to 30 mm.

One realization of storm intensities for each of the two synthetic storm events was used to develop variogram models. For the observed (real) storm event, the total depths of rainfall on all the gauges were used to develop a variogram. These variogram models were used in the interpolation process using kriging techniques. Multiquadric techniques were also applied to the three (two synthetic and one real) data sets. The cross-validation statistics and selected geometric parameters were then compared for both kriging and multiquadric interpolated rainfall fields.

Synthetic storm geometry for the synthetic storms was computed using the model of Rodriguez-Iturbe et al. (1987) developed from Walnut Gulch data;

$$z = \alpha \, e^{-2a^2 r^2} \qquad (8)$$

where, z is the value of function at distance r from an arbitrary point, α is the value of function at $r = 0$ and a is a decay parameter. Two synthetic storms with radii (r) of 3630 and 1950 m (designated storms 1A and 2A) centered over raingauges 33 and 40 (see

Fig. 2) were generated using $\alpha = 14$ mm/h (Fennesey, 1986), and $z = (0.01\alpha)$ at $r = 3630$ and 1950 m, respectively. Using these parameters, Eq. (8) was used to derive values at every raingauge within the two storm areas. The analytically derived values at the raingauges were then input into the interpolators to estimate values on a 100 m grid. Geometric storm measures such as cell volume were then computed numerically from interpolated values. These were compared with those computed analytically using Eq. (8) directly.

Once, it was observed (as described in Section 5) that the two procedures produced similar results, multiquadric interpolation was applied to the 304 events for computation of geometric parameters of storms. The value to be interpolated, $z(xi)$ was a 10-min rainfall depth (or intensity) at a given location x and a given time i. These values were treated independently (i.e. no particular relationships forced when considering all the $z(x)$ belonging to same rainfall event, lasting a duration d). In other words, interpolation method did not know which of the storm event a particular set of rainfall values to be interpolated belonged to. There is no relationship between the MQ parameters and the time of measurement/duration of storm. The relationship between the kriging parameters and the time of measurement/duration of storm etc. enters into the interpolation procedures via the variogram parameters, which depend on the spatial properties of the phenomenon to be interpolated.

Experimental directional variograms for the synthetic and observed storms were developed at an incremental angle of $22.5°$ with as much directional tolerance. The maximum distance in the variogram calculation was kept at 8000 m to insure that the number of pairs within the lag intervals was sufficient to estimate variogram parameters. For the synthetic storm cases the variogram plots were relatively scattered. But as one would expect from the symmetrical rainfall field, no directional anisotropy was prominent. Thus variogram parameters were adopted from omnidirectional variograms. For the observed storm case, the program 'GEOEAS' was used to compute variogram values using the total rainfall depths on all the gauges that reported rain during the storm event. Variogram values as a function of distance were then plotted to obtain the scatter plot

of variogram (the experimental variogram). An exponential model was fitted to the experimental variogram with a sill of 55 mm^2 and a range of 7500 m. We term this variogram as an 'event variogram' (as it was developed using data from a particular storm event). We also used another variogram to interpolate data from the observed storm event. This variogram model was adopted from the work of Tian (1993), and we termed it 'average variogram'. Tian (1993) used all the monthly data in the individual months within a 10-year period to develop monthly variograms. Variogram parameters such as model type, range and sill were taken directly from Tian's work. The purpose was to assess if there was any improvement in the cross validation statistics when individual event variogram model is used compared to using average monthly variogram parameters.

In the cross validation technique, the data locations are systematically suppressed one at a time and the value at that location is predicted using only the remaining data locations via interpolation. A variety of cross validation statistics using observed and estimated values are used to assess the performance of the interpolation methods. We used these statistics to evaluate and compare the performance of kriging and multiquadric methods. The cross validation statistics used in this study were those suggested by Hevesi (1992) and Cooper and Istok (1988), and are described below.

Percentage average estimation error (PAEE) assesses the unbiasedness of the interpolators. Estimates are considered unbiased if the PAEE is close to zero:

$$\text{PAEE} = \frac{100\%}{\overline{Z}_i n_i} \sum_{k=1}^{n_i} [Z_i^*(x_k) - z_i(x_k)] \qquad (9)$$

where, $Z_i^*(x_k)$ is the estimated value at location x_k, $z_i(x_k)$ is the deleted sample value, n_i is the total number of samples deleted, and $\overline{z_i}$ is the sample mean.

Another measure of the performance of the interpolator is the mean squared error (MSE). Cooper and Istok (1988) point out that the goal of the interpolation method should be to minimize the MSE. Furthermore, if the MSE is less than the variance of the sample values, then the interpolated estimates are

better than the mean of all the sample values.

$$\text{MSE} = \frac{1}{n} \sum_{i=1}^{n} [Z_i^*(x_k) - z_i(x_k)]^2. \qquad (10)$$

Estimates are considered accurate if the relative mean square error (RMSE) is close to zero:

$$\text{RMSE} = \frac{1}{s^2 n_i} \sum_{k=1}^{n_i} [Z_i^*(x_k) - z_i(x_k)]^2 \qquad (11)$$

where, s^2 is the sample variance.

Also computed were the minimum and maximum percentage errors.

3. Geometric measures

To compute geometric storm characteristics only those storms occurring from 1975 to 1991 with five or more gauges reporting with an average precipitation depth greater than 5 mm were considered. A total of 2604 rainfall events occurred during the period under study (1975–1991). Out of these, majority of the 'events' reported negligible amount of rain or rain on a very limited area. We wanted to avoid such events because data from a sporadic shower of rainfall on a single raingauge does not provide information about the spatial structure of rainfall. There are about 90 raingauges in an area of about 148 km^2 or one gauge for about 1.6 km^2. In that sense five gauges represent an area of about 8 km^2. This figure is very close to the average areal extent of storm cores (9 km^2) reported by Syed (1994). Moreover, fewer than 10% of the runoff events result from average rainfall depths less than 5 mm (Syed, 1994). Given these considerations we imposed a threshold of 5 mm and five gauges for selection of storm events. The number of storms meeting this criterion was 481 (out of a total of 2604). Next, we wanted to study only summer storms because they produce majority of runoff (about 90% according to Osborn and Lane, 1969). This reduced the number of storms of interest to 304. A storm event is defined to start after a lapse of at least one hour of no rainfall on any of the gauges in the watershed. Rainfall data are recorded as accumulated rainfall depth in uneven time intervals. These uneven time intervals are called breakpoints (so called

because they represent times when rainfall intensity changes). Breakpoint data from 91 gauges was used to estimate rainfall depths (total and at 10 min intervals) at every grid node (at a 100 m regular interval) forming a body defined in space which we term a rainfall 'cell'. The cell volume and the centroid can then be computed via summation of the interpolated values over the grid. Note that in the limit, as the grid mesh goes to zero, this is equivalent to block kriging and in the case of multiquadric it would correspond to analytic integration of the interpolating function.

Similar measures were computed for the core of the storm with 10 min rainfall intensities greater than 25 and 50 mm/h (core25 and core50). The storm core theoretically refers to that portion of storm, which is taken to produce runoff. The threshold values for its intensity are defined differently by different authors. For example, Koterba (1986) takes the core intensities to be 0.01 in/min (15 mm/h). Osborn and Lane (1969) take runoff producing precipitation to be greater than 0.4 in/h (10.2 mm/h). Simanton et al. (1983) tested the adequacy of the SCS (soil conservation service) curve number for predicting runoff from rangeland watersheds. They selected three intensity classes to include the range of observed maximum 15-min rainfall intensities. The classes had values ranging from 0.25 in/h (6.35 mm/h) to as high as 4.4 in/h (112 mm/h). Considering these studies, the 25 mm/h threshold was selected as it provides a conservative estimate for intensities which are very likely to produce runoff and the 50 mm/h threshold was selected to focus on the high intensity storm cores.

The straight line distance from the centroid projected on the watershed plane to the watershed outlet was termed 'distance from the outlet'. The areal coverage of the storm and storm cores was found by summing up areas of all the pixels having an interpolated total depth above a threshold of 0.25 mm, which is the effective measurement resolution of the raingauges. There are a number of livestock ponds within the watershed, which typically retain most of the water draining from their respective contributing areas (see Fig. 1). In other words, these ponds prevent water (running off from their respective contributing areas) from reaching the watershed outlet unless the ponds are full and overflowing. The contributing areas of these ponds were thus excluded

while computing storm geometric measures over individual watershed and nested subwatersheds when they had to be related (in a statistical sense) with the basin runoff.

4. Antecedent watershed and channel wetness

To assess the influence of antecedent watershed and channel wetness, several measures were defined in the following manner. The total amount of rainfall on all the gauges for each of five days prior to the event in question was obtained from the database. The soil moisture resulting from the rainfall totals was assumed to decay with time according to an exponential decay function (Faurès, 1990),

$$\Phi = \Phi_o \exp[\alpha t] \tag{12}$$

where, Φ is the soil moisture remaining in the soil from an initial moisture of Φ_o after a lapse of t hours. Personal communications with the personnel involved in field research (e.g. Roger Simanton) in this watershed suggested that most of the water in the first few centimeters of soil disappears in about five days. Thus with the assumption that only 10% of moisture remains in the top few centimeters of soil (i.e. $\Phi = 0.1\Phi_o$ at $t = 120$ h), the coefficient α in Eq. (12) was found to be -0.021. Eq. (12) was then backsolved for the 4th, 3rd, 2nd and the first prior day to determine the respective decay multipliers ($\exp[\alpha t]$). The decayed rainfall totals for the five prior days were then summed up to find the watershed wetness defined by individual gauges. These values were then used in the interpolation scheme to obtain a basinwide spatial description of antecedent watershed wetness. The centroidal height of this representation of wetness was computed. The area common to antecedent wetness and the concerned storm was identified and termed 'area of intersection'. A product of the value of the centroidal height of watershed antecedent wetness and the area of intersection was used in the correlation analysis as a measure of degree and extent of antecedent watershed wetness. Another measure of influence of antecedent watershed wetness was computed by adding the decayed prior rainfall totals to the rainfall in question. By doing that the rainfall in the area of intersection (between prior rainfall area and the area

of the rainfall in question) gets incremented by the total decayed prior rainfall.

If a runoff event occurs not long after a preceding runoff event, the channel wetness caused by the former may impact the gauged runoff total and peaks of the latter. A methodology similar to the treatment of antecedent watershed wetness as mentioned above was used to assess the impact of antecedent channel wetness. Runoff totals for five prior days were found for every runoff event. These totals were decayed by the same decay multipliers as described above. The decayed runoff totals provided an indication of antecedent channel wetness. They were used in the stepwise multiple correlation exercise to assess the importance of prevailing channel wetness (at the onset of storm in question) on runoff generation.

4.1. Relationship of antecedent wetness and storm properties to runoff

The two measures of antecedent watershed and channel wetness were used as independent variables in a stepwise multiple linear regression exercise along with other major geometric storm variables including total precipitation volume, the distance of storm cell from the outlet, the areal coverage, the maximum and mean intensities and duration. The runoff volume and the peak rate of runoff were used as dependent variables one at a time. The exercise was repeated for the storm core cases. The independent variable with the highest correlation with the dependent variable was first introduced in the regression model. The coefficient of determination (R^2) was observed. With this independent variable being kept in the model, each of the remaining variables was introduced in turn. The independent variable effecting the largest increase in the coefficient of determination was then kept in the model and the remaining variables were introduced one at a time.

5. Comparison of interpolation methods

As stated above, the comparison between interpolation methods was mainly done using cross validation technique. As mentioned above, cross validation techniques on two synthetic (assuming a central intensity of 14 mm/h) and

Table 1
Summary statistics for cross validation results (values interpolated are storm intensities)

Statistics	Test storm 1A		Test storm 2A		Storm of July 30, 1989		
	MQ	Krig	MQ	Krig	MQ	Kriging	
						Evt. var.	Avg. var.
PAEE	−0.06	−0.09	−0.24	−0.29	−0.57	−0.49	−0.91
MSE	0.57	0.61	2.04	2.19	26.62	24.81	34.67
RMSE	0.04	0.05	0.11	0.14	0.57	0.52	1.31
Minimum (%)	2.96	1.04	67.88	59.54	0.05	0.07	0.06
Maximum (%)	258.74	263.56	1686.59	2206.43	171.82	169.83	98.37

Avg. var. refers to the mean monthly variograms developed by another researcher using a 10-year data set from the same watershed. Evt. Var. refers to the variogram developed using rainfall intensity data from the specific storm under consideration.

one observed storm event were used (The values interpolated are the total storm intensity (mm/h) i.e. depth of rainfall on individual gauges divided by the duration of rainfall). The summary statistics are listed in Table 1. The results from the synthetic (test) storms may indicate that MQ is slightly better than Kriging but the opposite appears to be true for the observed storm case, which used the event variogram for kriging. Based on the cross validation results, no general conclusions can be drawn about the superiority of either method.

For the same analytical event cases, an examination of computed geometrical parameters shows that the values of cell volume and distance from the outlet were comparable (Fig. 3(a)). The largest differences occurred in estimation of areal coverage of the function when all gauges were used in the interpolation (Fig. 3(a)). Both kriging and MQ overestimated the area. Proper delineation of the area requires that the boundary of zero rainfall be properly interpolated. This is a common problem for many interpolation methods that they estimate small rainfall values outside the 'actual' rainfall extent. Therefore, interpolation methods were also assessed by using only those gauges reporting some rain (i.e. non-zero values), and by utilizing a threshold on the interpolated values. In this method, the only gauges reporting some rain are used. Rest of the gauges (i.e. zero gauges) are discarded. In other words, it is assumed that the network of gauges consists of only non-zero gauges. Obviously, different set of gauges report

rain from event to event. Therefore, the dimension of MQ matrix (see Eq. (5)) varies from storm to storm.

When only those gauges with nonzero rainfall were used in the computation, the MQ values for the areal coverage closely approximated the true values but kriging values were worse than the previous case (Fig. 3(b)). This was also reflected in the cell volume, which was overestimated by kriging. In the third case, a threshold of 0.25 mm (the effective raingauge measurement resolution) was applied to the interpolated values and all raingauges (whether reporting rain or not) were used in the interpolation. In this case, all interpolated values less than this amount were set equal to zero. This approach proved fruitful and both kriging and MQ estimates of the parameters were quite close to the analytic values (Fig. 3(c), Table 2, 'screened' case). Given these results, in all the subsequent computations, all gauges were used and a post interpolation threshold was applied on estimated values. Kriging theory offers a thresholding method called indicator kriging (Journel, 1978). Additionally, a method for delineating rainfall fields is provided by Barancourt and Creutin (1992). In their method, the zero rainfall is represented by binary random function. The rainfall variability inside the rainy areas is represented by an intrinsic random function. We used the threshold (screening of interpolated values) approach that provided best results for areal coverage of storms. Another reason for selecting the threshold approach
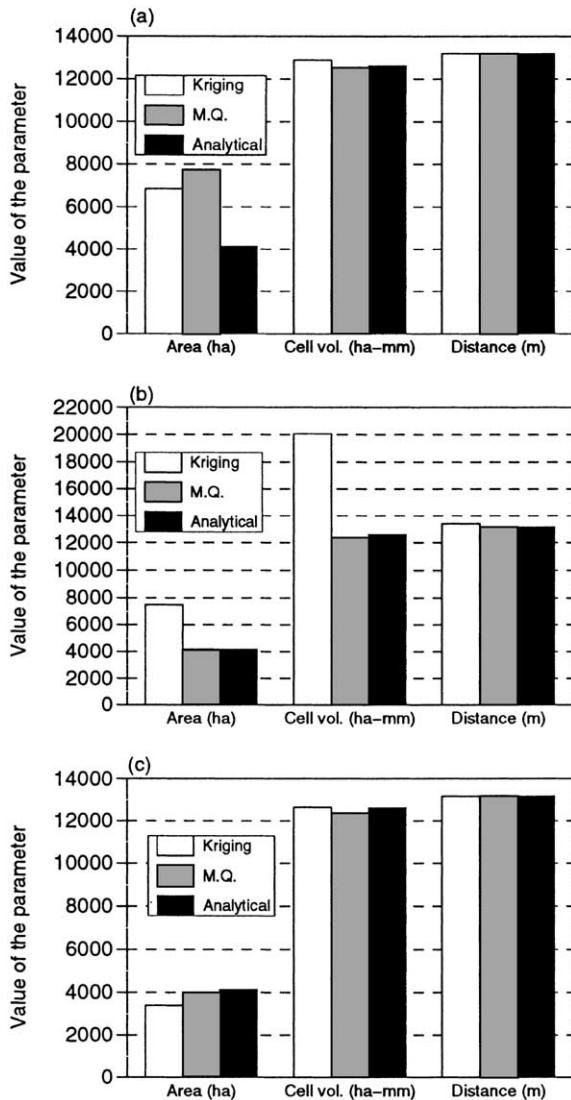
Fig. 3. Comparison of kriging and multiquadric computed parameters (storm area, storm cell volume and distance of storm core from the outlet) with the analytically derived values of these parameters (using analytic storm 1A): (a) All gauges including zero gauges used in the computation. (b) Only rain-reporting (non-zero) gauges used in the computation. (c) All gauges used in the computation and interpolated values screened (i.e. interpolated values which were less than 0.25 mm were screened out).

is that by using all gauges in the interpolation a non-variable (from storm to storm) number of system equations is attained. In other words, the MQ matrix has not to be changed from event to

event. This results in greater ease of implementation for processing a large data set.

For the observed storm case (storm of July 30, 1989), the same evaluation statistics were computed for interpolation by MQ as well as kriging which employed an average and event variogram (as described in Section 2). The cross validation statistics are summarized in Table 1. Using the average monthly variogram for kriging clearly produced inferior interpolation as compared to employing a variogram derived for the individual events. The cross-validation results for MQ and kriging (using the event variogram) are very comparable. Also, for the two synthetic storms, most of the statistics compare very well except that MQ underestimated more than kriging. The high maximum percentage differences for both MQ and kriging are probably the result of the fact that the synthetic rainfall surfaces are very steep (maximum intensity of 14 mm/h in the middle and decreasing to zero after a distance of 3630 and 1950 m for test storms 1A and 2A, respectively). Both the techniques failed to accurately define the steep gradients.

In terms of spatial geometric parameters, for the observed storm, there was little difference between MQ and kriging results, with the maximum difference between kriging and MQ of 1.4% for areal coverage; 0.005% difference in storm volume; and, 0.2% difference in storm centroidal distance from the outlet.

On the basis of the above results it was concluded that both MQ and kriging with a variogram derived for an individual event produce comparable interpolation results for the test cases examined. This observation reaffirms the observation of Borga and Vizzaccaro (1997) that estimates obtained by multiquadric were closer to those obtained by kriging for dense gauge networks. Given this conclusion, the remaining analysis was conducted using the MQ method.

6. Space–time rainfall cell characteristics

A histogram of total interpolated rainfall volume for all storms illustrates a typical positively skewed distribution of rainfall volumes (Fig. 4). The histogram

Table 2
Comparison of computed spatial parameters with true parameter of analytic surfaces

Case	Areal coverage (ha)					Cell volume (ha mm)					Distance from the outlet (m)				
	True	Krig	%d	MQ	%d	True	Krig	%d	MQ	%d	True	Krig	%d	MQ	%d
Unscreened															
Storm 1A	4139	6859	65.7	7761	87.5	12,637	12,900	2.1	12,542	−0.75	13,183	13,181	−0.02	13,198	0.12
Storm 2A	1194	4361	265.1	4188	250	3631	5134	41.4	4389	20.9	11,592	11,658	0.57	11,602	0.09
Screened															
Storm 1A	4139	3403	−17.8	4008	−3.2	12,637	12,666	0.23	12,392	−1.9	13,183	13,193	0.07	13,200	0.13
Sorm 2A	1194	1458	22	1658	38.8	3631	4975	37	4307	18.6	11,592	11,660	0.59	11,608	0.14

%d = (Krig. or MQ minus True)/(Krig. or MQ)100.

of areal coverage, on the other hand, is much different in nature (Fig. 5). A little less than half the total number of storms considered, occupy the entire watershed area. This often occurs due to the fact that storm events (as defined for data base reduction and treated in this study) are generally of long duration (mean = 285 min, SD = 179.3 min). Generally the entire watershed was not under rain at any given time, but when considering the entire event duration, large areas of the watershed receive rainfall during the event. This may be either due to physical storm motion within its

duration or due to multiple storm cells within an event, which should typically be considered as independent storms.

An interesting relationship of areal coverage of storm as a function of time was also observed (Fig. 6 red lines). To compute such a relationship, all the storms were given a start time of zero irrespective of their actual start time. The areal coverage of storm cell was computed every 10 min for every storm. Then the arithmetic average of the values was computed to find the mean of areal
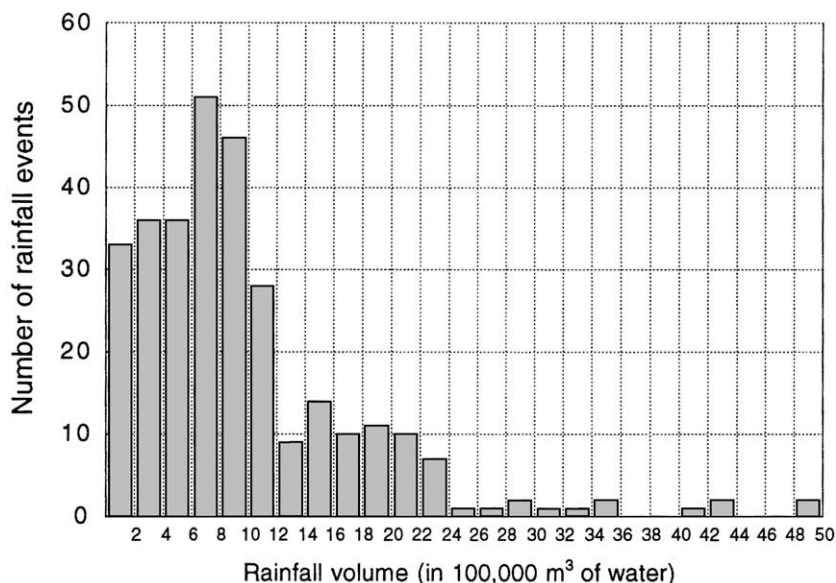

Fig. 4. Histogram of average rainfall volume (rainfall volume are computed by multiplying the interpolated rainfall intensity at every pixel (in m/h) with the area of the pixel (10,000 m^2) and then summing over all the pixel within the watershed and over the entire storm duration).
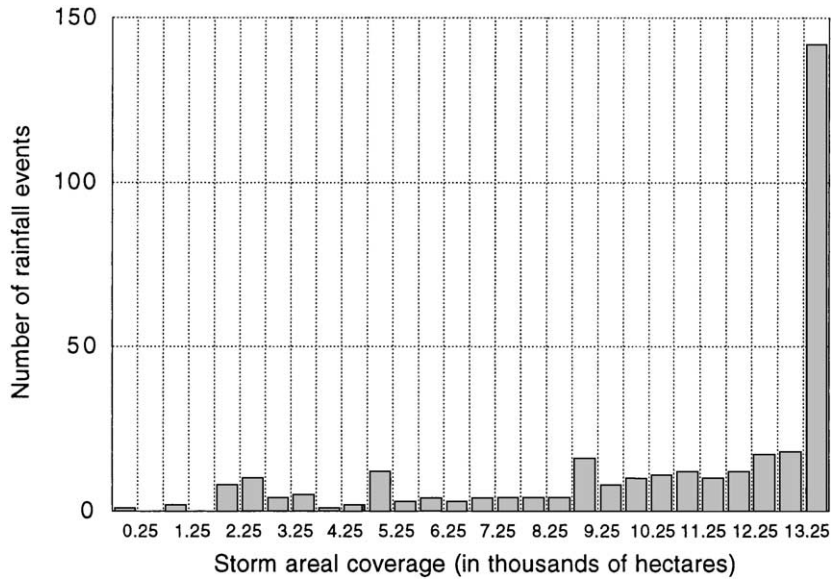
Fig. 5. Histogram of average areal coverage of storm (storm areal coverage is determined simply by adding area of all the pixels which have a non-zero interpolated rainfall).

coverage over all storms for every 10 min interval. The plot of areal coverage against time (Fig. 6 solid red line) shows that storms grow in area for about one and a half hours and then their areal coverage begins to decline. Note that the maximum mean areal coverage *at a given time step* is less than 7000 ha (roughly half the watershed). When

storm events are considered as a whole, however, the entire watershed could be covered (as mentioned above in the description of Fig. 5). This illustrates that although storms may cover the whole watershed, it is not likely that the whole watershed be covered with rain during the entire storm duration. A plot of mean storm position with
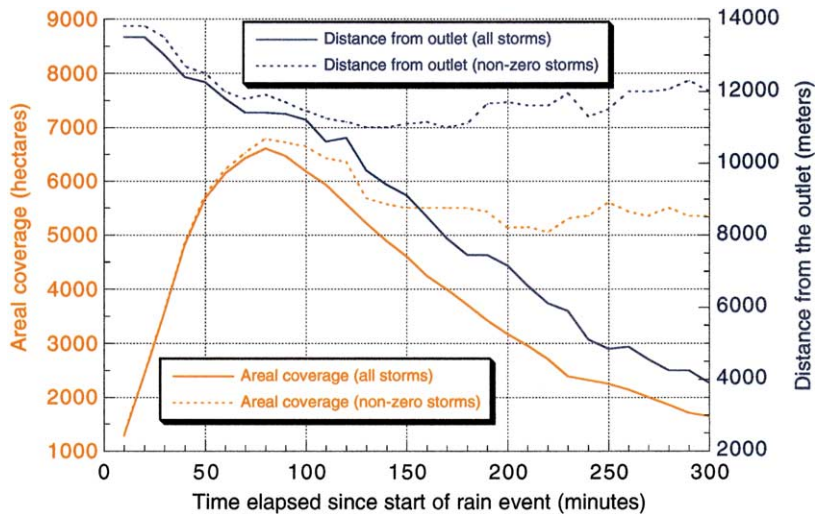

Fig. 6. Plot of average areal coverage and position of storm centroid versus elapsed time since start of rainfall. This plot illustrates how (on average) storms develop with time and the movement of storm centroid during storm duration.

time is also depicted in the same figure (Fig. 6). The plot (blue lines) illustrates that during the course of storm, the average 10-min-interval centroidal position drifts toward the watershed outlet for the first two hours (dashed blue line showing average for only non-zero values). This is the time interval in which majority of rainfall volume occurs. Also notice that (using only non-zero rain intervals) the average position is roughly at a distance of 12,000 m. This distance from the watershed outlet falls in the middle portion of the watershed (Fig. 2), which indicates that storm centers tend to fall in the middle region of the watershed. This will be discussed in more detail in Section 7 in relation to the significance of storm position for runoff generation.

7. Relationship of geometric storm measures with basin runoff

This study was undertaken with the premise that use of detailed storm characteristics and antecedent catchment characteristics will provide simple measures that will explain a high degree of runoff variability. It was postulated that in this region of highly spatially variable rainfall a relationship between storm occurrence and catchment size exists. Assuming random storm occurrence, a smaller catchment in a given region is less likely to receive rainfall than a larger catchment in the same region. But once a storm occurs in a smaller catchment it is more likely to cover proportionally more area of the catchment than that of a larger catchment. This is illustrated in Fig. 7 which plots the mean value and frequency of occurrence of the proportion of the storm to catchment area (A_{st}/A_{cat}) and the core area (defined as the portion of the storm having intensities greater than 25 mm/h) to catchment area (A_{core}/A_{cat}) versus the catchment size for all the 12 primary subwatersheds for all 304 storm events. As mentioned earlier, a storm event was defined over the entire Walnut Gulch watershed. The mean values were computed two ways; first, using all the data including any zero values (A_{st} or $A_{core} = 0$) and second, by considering only the non-zero values. It can be observed that, in general, as the watershed area increases the ratios decrease (Fig. 7 upper panel). This is true for both storm and core
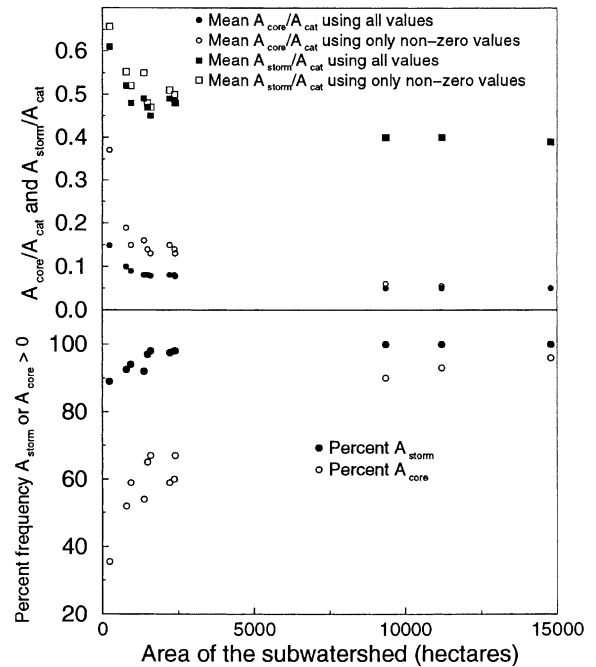

Fig. 7. Variation of relative storm and storm core areal coverage with catchment size. The top panel illustrates that larger the catchment size smaller the proportion of area covered by rainfall. Also notice that high intensity cores are limited in area (roughly the storm cores are about 4–8 times smaller than the overall storm).

ratios and for both methods of calculation of ratios (using all values and using only non-zero values). This observation shows that as the watershed area increases, in general, proportionally smaller and smaller area of the watershed gets covered by the storm (and storm cores).

Now, consider the vertical separation between solid and hollow squares (and circles) for a given size of the watershed. A large separation between solid and hollow squares (and circles) represents a large difference between the number of total and non-zero events (and cores). Now, notice the diminishing separation between solid and hollow squares (and circles) as the watershed area increases. (Obviously, for the largest of the watersheds, there is no non-zero event and thus no difference between the ratios calculated two ways: therefore, the solid and hollow markers fall in the same place.) This shows that as the watershed area decreases then it becomes less and less likely for that watershed to receive rain for a given rainfall event (defined on the basis of raingauges on

the largest watershed). In other words, the difference between the number of zero and non-zero events increases as the subwatersheds become smaller and smaller. The areal extent of storm cores are even more limited and thus the ratios are even smaller with a greater relative decrease in frequency of occurrence over a given catchment as the catchment size decreases. (Notice greater separation between solid and hollow circles than that between solid and hollow squares.) Therefore the use of spatial data for identification of storm cores becomes even more important as the catchment size increases.

The importance of areal storm core coverage is reflected in the relatively high correlation with runoff volume and peak rate as compared to total storm areal coverage. The correlation coefficient between core areal coverage with runoff and peak rate was 0.55 and 0.63 and only 0.19 and 0.15 for total storm areal coverage. This reiterates the importance of rainfall intensities in runoff generation as opposed to total rainfall depths in this infiltration excess dominated runoff environment. The volume of rainfall associated with the storm core was accordingly much better correlated with runoff volume and peak rate (a correlation coefficient of 0.71 and 0.76, respectively) as compared to total precipitation volume (a correlation coefficient of 0.59 and 0.53, respectively). The scatter plot of rainfall (core25) volume versus the runoff volume is presented in Fig. 8. Similar correlations were developed using only a single raingauge to illustrate the additional information

acquired with spatial data. We selected a raingauge, which visually appeared to be near the center of gravity of the watershed (gauge 40, see Fig. 2). We selected a gauge near the middle portion because such a gauge would generally be taken to represent the rainfall received by the watershed better than a gauge (say) near the boundary. The correlation of the storm core rainfall volume with runoff volume was 0.71 for the spatial data and 0.60 for the central gauge data (0.66 and 0.64, respectively for the total storm rainfall volume).

The correlation statistics alone can mask the critical importance of spatial rainfall information. This point is illustrated with an example in Fig. 9 for the storm of 2nd September 1988. The average rainfall intensity using all gauges obtained via interpolation and the rainfall intensity on a single central gauge are plotted as a function of time. We selected a single central raingauge, which is visually located in the middle portion of the watershed. We did this because gauges in the middle of the watershed are generally taken to represent rainfall better than the gauges (say) near the watershed boundary. Runoff from WG6 is also plotted. It can be seen that the rainfall reported by a central gauge poorly represents the overall rainfall situation as the runoff started before the rainfall began on the central gauge. On the other hand the rainfall intensity computed using all gauges corresponds markedly better to the runoff. Even at the 4.4 ha scale within this environment Goodrich et al. (1995) and Faurès et al. (1995) noted
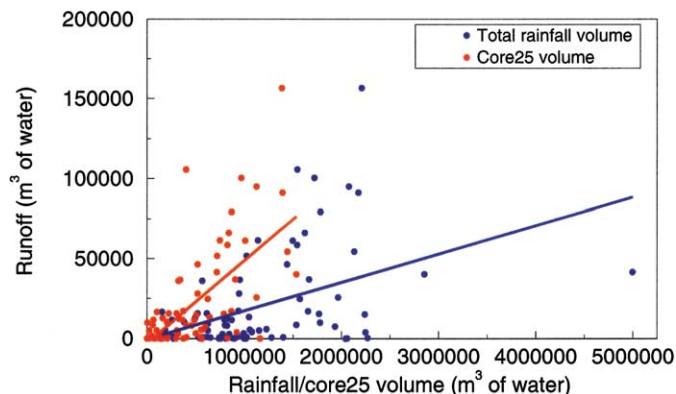

Fig. 8. The scatter plot of rainfall (core25) volume versus the runoff volume for all runoff producing storms. The coefficient of correlation between core25 volume and runoff is 0.71 and between the total volume of rain and runoff is 0.59. Notice that the runoff produced by some of the storms is of negligible magnitude.
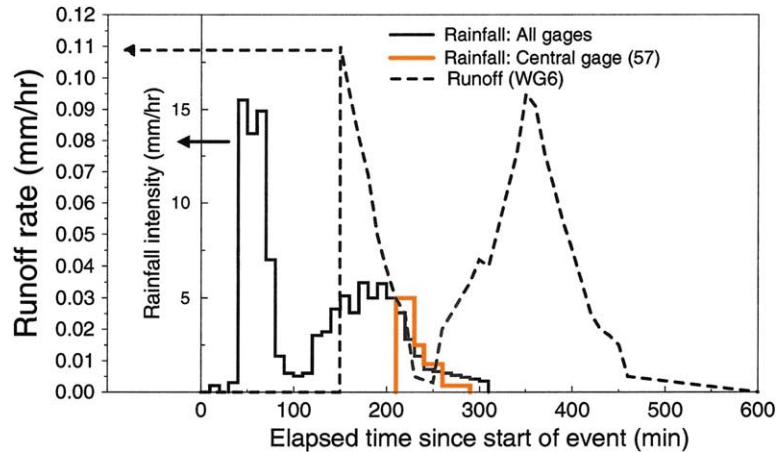
Fig. 9. Advantage of using spatially distributed rainfall information: an example. The illustration shows that a single raingauge can misrepresent the amount of rainfall received by the watershed.

significant spatial rainfall variability and that using spatial rainfall data from multiple gauges significantly improved runoff predictability.

This study also indicated that the position of the storm or the storm core within the watershed is virtually uncorrelated with the runoff volume or peak rate when the entire Walnut Gulch watershed is considered. The correlation coefficient between centroidal distance of overall storm from the watershed outlet was estimated to be -0.01 and 0.01 for runoff volume and peak runoff rate, respectively (-0.05 and -0.04 using storm cores). But Osborn (1964) had speculated that where the storm is centered should become increasingly important with increasing watershed size due to channel losses in this ephemeral watershed (Renard et al., 1993). The virtual uncorrelation of the storm or the core distance with the runoff volume or the peak rate of runoff *when the entire Walnut Gulch watershed is considered* can be explained as follows.

In an attempt to investigate the relationship of storm distance from the outlet to runoff volume without the watershed shape bias another exercise was undertaken considering nine subwatersheds which range from 635 to 12,736 ha. To obtain a comparable set of storms only those storms for which the ratio A_{core}/A_{cat} was within 0.02–0.10 were used. For each of these storms the ratio of observed subwatershed runoff over core storm volume was computed (a measure of basin attenuation). This

ratio is obviously zero for those events, which did not produce any runoff. The mean of these values were plotted against the mean distance of the storm core from the respective outlet (see Fig. 10). This plots tends to confirm the suggestion by Osborn (1964) that storm position will be a factor in runoff generation. Across the watersheds it can be observed that as the mean distance of the core from the outlet increases, on average, a lesser amount of runoff is generated for a given rainfall core volume. Also for a given watershed, there is a general trend that runoff producing storms have storm cores closer to the respective watershed outlet and this trend is more pronounced as the watershed area increases (notice the increasing horizontal separation of mean distance between runoff producing and all-storms cases as the watershed size increases). This observation emphasizes importance of the scale of interaction between catchment and storm geometries.

It can be observed from the histogram of distance from the outlet (Fig. 11) that more than half of the storms have their centroids located in the range from 8000 to 11,000 m. This range of distance falls near the middle portion of the watershed (see Fig. 2). This is also illustrated in Fig. 12 in which total storm coverage is plotted against the storm distance from the outlet. Most of the points cluster between 9 and 14 km distance. Most of the points covering the entire watershed also fall in this range. This distribution of
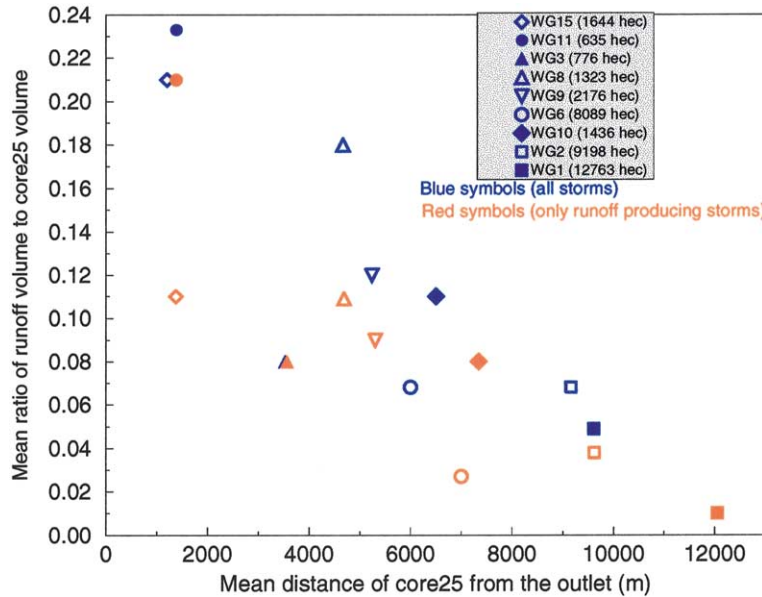
Fig. 10. Plot showing the attenuation of core25 volume as a function of size of the catchment over a range of basin scales.

the number of storms and the areal coverage indirectly mimics the distribution of watershed area as a function of distance from outlet (see Fig. 13). The shape of the watershed is such that relatively more area (in the north–south direction) is concentrated in the middle portion with tapering geometry in towards the east and the west (see Fig. 2). Fig. 13 illustrates this by plotting the watershed area falling between successive equidistant imaginary radial lines emanating from the outlet of the watershed as a function of distance from the outlet to the center of the radial lines. We see that there is concentration of watershed area in the middle region (like a normal distribution

curve). In this situation, storm distance from the outlet is a biased parameter. Assuming random storm location, increased sampling or storm occurrence takes place in the larger central portion of the watershed. The large number of samples (storms) occurring within distances of 9–14 km influences the regression so that storm close to or far from the outlet are effectively not given equal emphasis. This bias makes this parameter incapable of serving as surrogate for channel losses in regression analysis.

Fig. 12. Storm areal coverage versus distance from the watershed outlet. Notice the cluster of points just above the 12,000 ha line. The maximum represents the total area of the watershed excluding pond catchment regions.
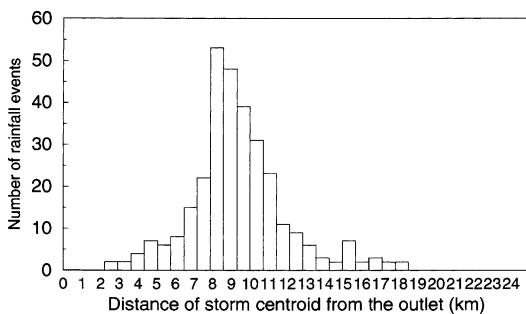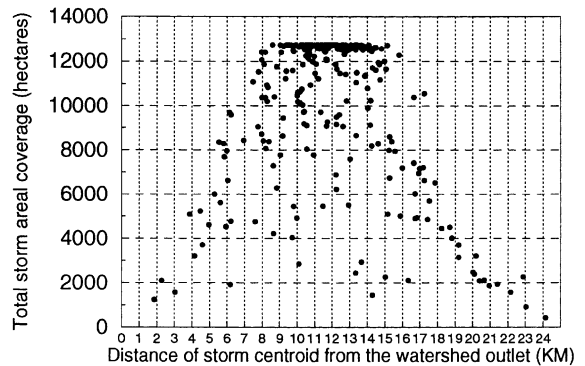

Fig. 11. Histogram of storm centroidal distance from the watershed outlet illustrating that majority of storms have their centroids in the range from 8–11 km.
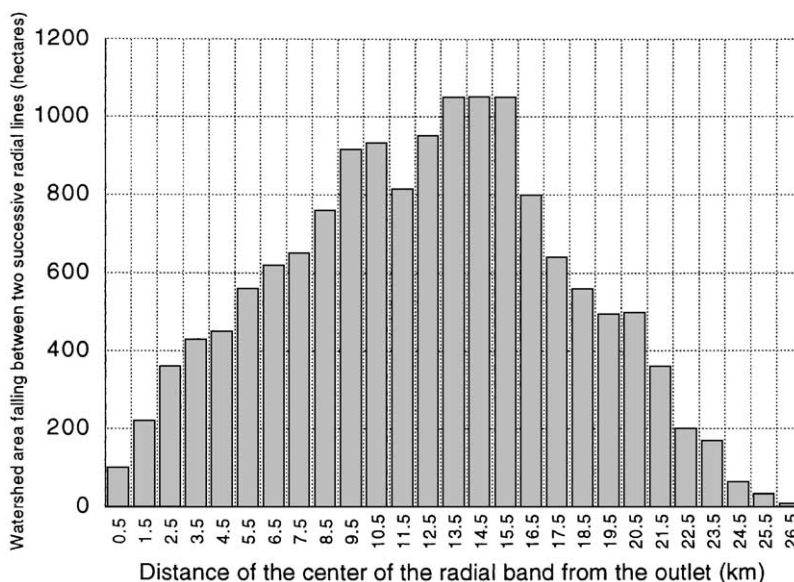
Fig. 13. The distribution of the watershed area as a function of distance from the watershed outlet. Notice concentration of area near the middle portion which results in bias when computing the centroids of portion of storms falling within the watershed boundary.

8. Regression results and antecedent watershed wetness

Step-wise multiple linear regression was used to assess relative importance of various geometric parameters and antecedent watershed (and channel) wetness as described in Section 3 and 4. The results are summarized in Table 3. Only results of first two steps of regression are presented because generally there was no substantial improvement with the introduction of any subsequent variables. For WG1 total precipitation volume accounted for only 35 and 28% of the variation in runoff volume and peak rates, respectively. An introduction of areal coverage and

Table 3
Regression coefficient of determination (R^2) for various independent variables

WS ↓	Dep. Var. ⇒ Ind. Var. ↓	Runoff volume			Ind. Var. ↓	Peak runoff rate		
		Tot st.	Core25	Core50		Tot. st.	Core25	Core50
WG1	V_p	35			V_p	28		
	$V_p + A_s$	41			$V_p + I_m$	37		
	V_c		51	52	V_c		58	67
	$V_c + A_{ch}$		53	55	$V_c + A_{ch}$		60	70
WG6	V_p	39			V_p	29		
	$V_p + A_s$	46			$V_p + I_m$	34		
	V_c		56	52	V_c		57	60
	$V_c + I_{mt}$		59	56	$V_c + A_{mt}$			62
WG11	V_p	30			V_p	24		
	$V_p + A_s$	36			$V_p + d_e$	32		
	V_c	52	57		V_c		46	52
	$V_c + A_c$	54	60		$V_c + A_{ch}$			

V_p: precip volume (m³), A_s: storm area (ha), V_c: volume of core (m³), A_{ch}: antecendent channel wetness, I_{mt}: maximum step intensity (mm/h), I_m: mean pixel intensity (mm/h), d_e: duration of event (min); A_c: area of storm core (m²).

duration in the model boosts the value of R^2 to 41% in case of runoff volume. Beyond that there was no improvement with the introduction of any other variables. The most important variable (other than precipitation volume) in case of peak rate is the mean intensity. There is a marked improvement in the regression coefficient when storm core volumes are considered. Core volume accounts for 51 and 58% of variation in runoff volume and peak rates, respectively. It is of interest to note that while the total volume of rain explains the runoff volume better than the peak rate, the core volume explains the peak rate better than the runoff volume. The antecedent channel wetness and the areal coverage are other important variables and with the introduction of these variables along with the core volumes the R^2 increases to 55 and 70% for runoff volume and peak rate, respectively. The regression results for WG6 are similar to WG1, however results for WG11 show some differences. For WG11 the precipitation volume explains only 30% of variation in runoff volume. Areal coverage of storm is the second most important variable and the two variables together explain 36% of the variation. The core volume alone, on the other hand, accounts for 52% of the variation. Although regression results are far from being conclusive, two observations are fairly apparent. First, the high intensity portions of the storm (the storm cores) seem to be responsible for much of the runoff than any other single variable. Second, the antecedent watershed and channel wetness as defined and treated in this study seem to be of secondary importance for controlling runoff volumes or the runoff peak rates. This is consistent with the fact that watershed soil moisture 'memory' is relatively short in this semiarid environment where potential evapotranspiration averages roughly 10 times annual rainfall.

9. Conclusions

The cross validation statistics for kriging and MQ residuals were found to be very similar for the test cases examined in this study. We alluded to the theoretical equivalence between the two methods above. The similarity of the cross validation statistics shows that the two methods produce similar results when variograms are developed using data from specific events. When long-term average monthly variogram parameters were used, kriging produced inferior results. Another reason for the similarity of results may be the fact that the raingauge network used in this study is very dense. Our results are similar to the results of recent studies, which reported that for high resolution networks kriging method did not show greater predictive skill than simpler techniques (e.g. see Dirks et al., 1998; Borga and Vizzaccaro, 1997).

The study showed that the interaction between catchment shape and the areal extent and position of storm is an important controlling factor for runoff generation. Storm centroidal distance from the outlet did not prove to be a good indicator of rainfall attenuation through the watershed when the entire watershed was considered. The regression analyses tend to bias the results because of the peculiar geometry of the watershed. But when the analysis was expanded to other smaller watersheds and the storm core was considered instead of the whole storm, it became apparent that the position of storm core becomes increasingly more important as the watershed size increases. Increasingly more rainfall volume attenuation was observed as the distance of the core from the outlet increased. This observation indicates that channel abstractions may be a very important factor controlling the basin response in the region of study; and, as Michaud and Sorooshian (1994b) pointed out that realistic estimation of channel losses requires estimates of the locations of partial contributing areas, it becomes even more important to account for spatial and temporal variability of rainfall in this region. The effort spent in this study to define rainfall input at a fine spatial and temporal resolution using a dense network of gauges provides some insight into value of using spatially distributed data over point data. In our opinion the sampling density plays an important role in better identifying and defining runoff producing storm cores.

The study also observed a relative minor importance of antecedent watershed or channel wetness as indicated by the regression analysis. The introduction of antecedent channel wetness provided some improvement in the explanatory power of the regression model only in the largest of the three watersheds studied (i.e. WG1). While antecedent watershed wetness did not improve the explanatory power of the model in any of the three watersheds. It

should, however, be mentioned that these two factors were treated in a rather simplistic manner in this study because of a lack of data. We believe that the issues related to watershed or channel wetness are complex in their nature and warrant more data and refinement of methods.

The study also showed that in an overall sense storms are generally large in areal coverage as compared to the extent of the Walnut Gulch watershed. The areal coverage of the storm core (which is usually much smaller in areal size) is, however, better correlated to the runoff than the areal coverage of the whole storm. Also the core volume of rainfall, defined as the volume of rainfall occurring above a threshold intensity of 25 mm/h explains more variation in runoff volume and the peak rate than other storm measures.

Acknowledgements

References

Abtew, W., Obeysekera, J., Dhih, G., 1993. Spatial analysis for monthly rainfall in south Florida. Water Resources Bulletin 29 (2), 179–188.

Amani, A., Lebel, T., 1997. Langrangian kriging for the estimation of Sahelian rainfall at small time steps. Journal of Hydrology 192, 125–157.

Barancourt, C., Creutin, J.D., Rivoirard, J., 1992. A method for delineating and estimating rainfall fields. Water Resources Research 28, 1133–1144.

Barendregt, L.G., 1987. Estimation of the generalized covariance when it is a linear combination of two known generalized covariances. Water Resources Research 23 (4), 583–590.

Bastin, G., Lorent, B., Duque, C., Gevers, M., 1984. Optimal estimation of the average areal rainfall and optimal selection of rain gauge location. Water Resources Research 20 (4), 463–470.

Borga, M., Vizzaccaro, A., 1997. On the interpolation of hydrologic variables, formal equivalence of multiquadric surface fitting and kriging. Journal of Hydrology 195, 160–171.

Cooper, R.M., Istok, J.D., 1998. Geostatistics applied to groundwater contamination. I: methodology. Journal of Environmental Engineering 114, 270–286.

Creutin, J.D., Obled, C., 1982. Objective analyses and mapping techniques for rainfall fields: an objective comparison. Water Resources Research 18 (2), 413–431.

Dirks, K.N., Hay, J.E., Stow, C.D., Harris, D., 1998. High-resolution studies of rainfall on Norfolk Island Part II: interpolation of rainfall data. Journal of Hydrology 208, 187–193.

Englund, E., Sparks, A., 1990. GEO-EAS (Geostatistical Environmental Assessment Software) user's guide. Environmental monitoring systems laboratory, office of research and development, US Environmental Protection Agency, Las Vegas, Nevada.

Faurès, J.-M., 1990. Sensitivity of runoff to small scale spatial variability of observed rainfall in a distributed model. MS Thesis, Department of Hydrology and Water Resources, University of Arizona, Tucson, Arizona.

Faurès, J.-M., Goodrich, D.C., Woolhiser, D.A., Sorooshian, S., 1995. Impact of small-scale spatial rainfall variability on runoff simulation. Journal of Hydrology 173, 309–326.

Fennessey, N.M., Eagleson, P.S., Qinliang, W., Rodriguez-Iturbe, I., 1986. Spatial analysis of storm depths from an Arizona raingauge network. Report No. 306, Ralph M. Parsons Laboratory, Hydrology and Water Resources Systems, Department of Civil Engineering, School of Engineering, Massachusetts Institute of Technology, Cambridge, Massachusetts.

Goodrich, D.C., 1990. Geometric simplification of a distributed rainfall–runoff model over a range of basin scales. PhD dissertation, Department of Hydrology and Water Resources, University of Arizona, Tucson, Arizona, pp. 361.

Goodrich, D.C., Faurès, J.-M., Woolhiser, D.A., Lane, L.J., Sorooshian, S., 1995. Measurement and analysis of small-scale convective storm rainfall variability. Journal of Hydrology 173, 283–308.

Goovaerts, P., 2000. Geostatistical approaches for incorporating elevation into the spatial interpolation of rainfall. Journal of Hydrology 228, 113–129.

Grayson, R.B., Moore, I.D., McMohan, T.A., 1992. Physically based hydrologic modeling, 2, Is the concept realistic? Water Resources Research 28 (10), 2659–2666.

Hardy, R.L., 1971. Multiquadric equations of topography and other irregular surfaces. Journal of Geophysical Research 76, 1905–1915.

Hevesi, J.A., Istok, J.D., Flint, A.L., 1992. Precipitation estimation in mountainous terrain using multivariate geostatistics. Part I:

structural analysis. Journal of Applied Meteorology 31 (4), 661–676.

Journel, A.G., Huijbregts, C.J., 1978. Mining Geostatistics, Academic Press, London.

Koterba, M.T., 1986. Differences influences of storm and watershed characteristics on runoff from ephemeral streams in southeastern Arizona. PhD dissertation, Department of Hydrology and Water Resources, University of Arizona, Tucson, Arizona.

Kruizinga, S., Yperlaan, G.J., 1978. Spatial interpolation of daily totals of rainfall. Journal of Hydrology 36, 65–73.

Kwaadsteniet, J.W., 1990. On some fundamental weak spots of kriging technique and their consequences. Journal of Hydrology 114, 227–284.

Lebel, T., Bastin, G., Obled, C., Creutin, J.D., 1987. On the accuracy of areal rainfall estimation: a case study. Water Resources Research 23 (11), 2123–2134.

Lee, P.S., Lynn, P.P., Shaw, E.M., 1974. Comparison of multiquadric surfaces for the estimation of areal rainfall. Hydrological Sciences, ÄXIXÄ(3) 9, 303–317.

Loague, K.M., Freeze, R.A., 1985. A comparison of rainfall runoff modeling techniques on small upland catchments. Water Resources Research 21 (2), 229–248.

Mandeville, A.N., Rodda, J.C., 1970. A contribution to the objective assessment of areal rainfall amounts. Journal of Hydrology 9 (2), 281–291.

Michaud, J.D., Sorooshian, S., 1994a. Comparison of simple versus complex distributed runoff models on a midsized semiarid watershed. Water Resources Research 30 (3), 593–605.

Michaud, J.D., Sorooshian, S., 1994b. Effect of rainfall sampling errors on simulations of desert flash floods. Water Resources Research 30 (10), 2765–2775.

Myers, D.E., 1991. Interpolation and estimation with spatially located data. Chemometrics and Intelligent Laboratory Systems 11, 209–228.

Myers, D.E., 1994. Spatial interpolation: an overview. Geoderma 62, 17–28.

Osborn, H.B., 1964. Effect of storm duration on runoff from rangeland watersheds, in the semiarid southwestern United States. International Association of Scientific Hydrology IX (4), 40–47.

Osborn, H.B., Lane, L.J., 1969. Precipitation–runoff relations for very small semiarid rangeland watersheds. Water Resources Research 5 (2), 419–425.

Pegram, G.C., Pegram, G.S., 1993. Integration of rainfall via multiquadric surfaces over polygons. Journal of Hydraulic Engineering 119 (2).

Reich, B.M., Osborn, H.B., 1982. Improving point rainfall prediction with experimental data? Int. Statistical Analysis of Rainfall and Runoff. International Symposium on Rainfall/Runoff, Mississippi State University, Water Resources Publication, P.O. Box 2841, Littleton, CO, pp. 41–54.

Renard, K., Lane, L.J., Simanton, J.R., Emmerich, W.E., Stone, J.J., Weltz, M.A., Goodrich, D.C., Yakowitz, D.S., 1993. Agricultural impacts in an arid environment: Walnut Gulch case study. Hydrological Science and Technology 9 (1–4), 145–190.

Rodriguez-Iturbe, I., Qinliang W., Jacobs, B., Eagleson, P.S., 1987. Spatial Poisson models of stationary storm rainfall: theoretical development. Ralph M. Parsons Laboratory Hydrology and Water Resources Systems. Department of Civil Engineering, School of Engineering. Massachusetts Institute of Technology, Cambridge, Massachusetts.

Seed, A.W., Austin, G.L., 1990. Sampling errors for raingauge-derived mean areal daily and monthly rainfall. Journal of Hydrology 118, 163–173.

Shaw, E.M., Lynn, P.P., 1972. Areal rainfall evaluation using two surface fitting techniques. Bulletin of International Association of Hydrological Sciences, XVII 12 (4), 419–433.

Simanton, J.R., Osborn, H.B., 1983. Runoff estimates for thunderstorm rainfall on small rangeland watersheds. Hydrology and Water Resources in Arizona and the Southwest. Proceedings of the 1983 Meetings of the Arizona Section, American Water Resources Association and the Hydrology Section, Arizona, Nevada Academy of Sciences, Flagstaff, Arizona, April 16.

Smith, R.E., Shreiber, H.A., 1973. Point processes of thunderstorm rainfall, 1 distribution of rainfall events. Water Resources Research 9 (4), 871–884.

Smith, R.E., Shreiber, H.A., 1974. Point processes of thunderstorm rainfall, 2 rainfall depth probabilities. Water Resources Research 10 (3), 418–426.

Supachai, S., 1988. Comparative studies of kriging, multiquadric-biharmonic and other methods for solving mineral resources problems. PhD dissertation. Department of Earth Sciences, Iowa State University, Ames, Iowa.

Syed, K., 1994. Spatial storm characteristics and basin response. MS Thesis. Department of Hydrology and Water Resources, University of Arizona, Tucson, Arizona.

Tabios, G.Q. III, Salas, J.D., 1985. A comparative analysis of techniques for spatial interpolation of precipitation. Water Resources Bulletin 3, 365–380.

Thiessen, A.H., 1911. Precipitation averages for large areas. A subsection in the Climatology data for July 1911, District No. 10, Great Basin, Monthly Weather Review, July: 1082–1084.

Tian, D., 1993. Rainfall spatial and seasonal variability analysis in semiarid watersheds. MS Thesis, Department of Hydrology and Water Resources, University of Arizona, Tucson, Arizona.

Woolhiser, D.A., 1996. Search for physically based runoff model—a hydrologic El Dorado? Journal of Hydraulic Engineering 122 (3), 122–129.

Woolhiser D.A., Smith R.E., Goodrich D.C., 1990. A kinematic runoff and erosion model: documentation and user manual, ARS 77, US Department of Agriculture.

Young, K.C., 1992. Three-way model for interpolating for monthly precipitation values. Monthly Weather Review 120 (11), 2561–2569.